Journal of Solid State Chemistry 182 (2009) 2096–2103

Contents lists available at ScienceDirect

Journal of Solid State Chemistry

journal homepage: www.elsevier.com/locate/jssc

Orthorhombic–orthorhombic phase transitions in $Nd_2NiO_{4+\delta}$ ($0.067 \leq \delta \leq 0.224$)

Kenji Ishikawa *, Kenji Metoki, Hiroshi Miyamoto

Department of Applied Chemistry, Meiji University, Higashi-mita, Tama-ku, Kawasaki 214-8571, Japan

ARTICLE INFO

Article history:
Received 30 September 2008
Received in revised form
12 May 2009
Accepted 17 May 2009
Available online 29 May 2009

Keywords:
$Nd_2NiO_{4+\delta}$
Phase transforms
Phase diagram

ABSTRACT

Variation of the phases of $Nd_2NiO_{4+\delta}$ with the excess oxygen concentration δ has been examined at room temperature in the range $0.067 \leq \delta \leq 0.224$ using the X-ray powder diffraction technique. The phases observed at room temperature are orthorhombic-I ($0.21 < \delta \leq 0.224$), orthorhombic-IV ($0.175 < \delta \leq 0.21$), orthorhombic-II ($0.15 < \delta \leq 0.175$), orthorhombic-II+quasi-tetragonal-I ($0.10 < \delta \leq 0.15$), and quasi-tetragonal-I ($0.067 < \delta \leq 0.10$).

1. Introduction

Only three oxides of $La_2NiO_{4+\delta}$, $Pr_2NiO_{4+\delta}$, and $Nd_2NiO_{4+\delta}$ are available as K_2NiF_4 type lanthanide nickel oxides, since the thermodynamic stability of the K_2NiF_4 type oxides is determined by the Goldshmidt tolerance factor associated with the ionic radius of the trivalent lanthanide cation. The stability of the K_2NiF_4 type oxides decreases with decreasing the tolerance factor and with decreasing the ionic radius of the lanthanide cation. Nickel oxides of La, Pr, and Nd can exist as K_2NiF_4 type oxides, while nickel oxides of lanthanide elements excluding La, Pr, and Nd cannot exist as K_2NiF_4 type ones but as perovskite type ones. A chemical feature commonly found in these K_2NiF_4 type oxides is the existence of the excess oxygen, the concentration of which is given by δ in the chemical formula. The excess oxygen of these oxides becomes a mobile ion at high temperature [1,2], and the oxides are oxide ion conductors. However, these oxides are classified in mixed electronic ionic conductors, because the electronic conductivity of each oxide is much higher than the ionic conductivity [3]. Electrochemical properties of $La_2NiO_{4+\delta}$, $Pr_2NiO_{4+\delta}$, and $Nd_2NiO_{4+\delta}$ are well investigated, and various applications are proposed.

On investigating the electrochemical properties and the applications of the oxides, phase diagrams of the oxides should be indispensable, because most properties of the oxides closely relate to their phases. The phases of the oxides should have been fully examined as functions of temperature and the excess oxygen concentration beforehand. However, only several oxygen phase diagram studies have been reported for $La_2NiO_{4+\delta}$ [4–12], $Pr_2NiO_{4+\delta}$ [13–20], and for $Nd_2NiO_{4+\delta}$ [21–32]. Some difficulty in preparing the samples with various excess oxygen concentrations may obstruct the phase diagram studies.

For the room temperature phases of $Nd_2NiO_{4+\delta}$, the followings are known. Puche et al. [21] have prepared a nearly stoichiometric sample of Nd_2NiO_4 and found that the sample is in orthorhombic *Bmab* symmetry with a large orthorhombic strain: $a = 538.14(5)$ pm, $b = 558.50(2)$ pm, $c = 1211.43(4)$ pm. Carvajal et al. [22] have also reported that the stoichiometric sample of Nd_2NiO_4 is in orthorhombic *Bmab* symmetry at room temperature but is in tetragonal $P4_2/ncm$ symmetry below 130–138 K [23–29]. Takeda et al. [30] have prepared eleven samples of $Nd_2NiO_{4+\delta}$ in the range $0.11 \leq \delta \leq 0.25$ and found that each sample is in orthorhombic *Bmab* symmetry in the range $0.11 \leq \delta < 0.13$ and in orthorhombic *Fmmm* symmetry in the range $0.13 \leq \delta \leq 0.25$. They also pointed out that while the orthorhombic strain of the *Bmab* sample is very small, the sample is apparently in orthorhombic symmetry. Bhavaraju et al. [31] have prepared seven samples of $Nd_2NiO_{4.00}$, $Nd_2NiO_{4.02}$, $Nd_2NiO_{4.04}$, $Nd_2NiO_{4.06}$, $Nd_2NiO_{4.08}$, $Nd_2NiO_{4.14}$, and $Nd_2NiO_{4.18}$ by electrochemical intercalation of oxygen into $Nd_2NiO_{4+\delta}$ at 298 K. They reported that $Nd_2NiO_{4.00}$ is in orthorhombic symmetry, $Nd_2NiO_{4.02}$, is a two-phase mixture of $Nd_2NiO_{4.00}$ and $Nd_2NiO_{4.04}$, $Nd_2NiO_{4.04}$, $Nd_2NiO_{4.06}$, and $Nd_2NiO_{4.08}$ are very close to tetragonal, $Nd_2NiO_{4.14}$ is a two-phase mixture of $Nd_2NiO_{4.08}$ and $Nd_2NiO_{4.18}$, and that $Nd_2NiO_{4.18}$ is in orthorhombic symmetry. Zaghrioui et al. [32] have prepared four samples of $Nd_2NiO_{4.049}$, $Nd_2NiO_{4.065}$, $Nd_2NiO_{4.077}$, and $Nd_2NiO_{4.234}$. They reported that $Nd_2NiO_{4.049}$ and $Nd_2NiO_{4.065}$ are two-phase mixtures of an orthorhombic *Bmab* phase and a tetragonal $I4/mmm$ phase, $Nd_2NiO_{4.077}$ is in tetragonal $I4/mmm$ symmetry, and that $Nd_2NiO_{4.234}$ is in orthorhombic

* Corresponding author. Fax: +81 44 934 7906.
E-mail address: kishikaw@isc.meiji.ac.jp (K. Ishikawa).

0022-4596/$ - see front matter © 2009 Elsevier Inc. All rights reserved.
doi:10.1016/j.jssc.2009.05.025

Fmmm symmetry. As shown above, the reports on the room temperature phases of $Nd_2NiO_{4+\delta}$ are not very consistent with each other, because the phase diagram of $Nd_2NiO_{4+\delta}$ should be much more complex than that expected from the above studies.

Although the room temperature phases of $Nd_2NiO_{4+\delta}$ have not been very well examined, the phases of $Pr_2NiO_{4+\delta}$ are completely investigated. Buttrey et al. [13] have prepared two samples of $Pr_2NiO_{4.020}$ and $Pr_2NiO_{4.060}$ and examined their phases with a neutron diffraction technique. They found that $Pr_2NiO_{4.020}$ is in tetragonal $P4_2/ncm$ symmetry below 118 K but is a two-phase mixture of the tetragonal $P4_2/ncm$ phase and the orthorhombic *Pccn* phase above 118 K, and that $Pr_2NiO_{4.060}$ is in tetragonal $P4_2/ncm$ symmetry in the range from 5 to 300 K. They also pointed out that space groups of *Bmab*, $P4_2/ncm$, and *Pccn* are Landau subgroups of the $I4/mmm$ space group. The orthorhombic *Bmab* structure is given from the parent $I4/mmm$ structure by rotating the NiO_6 octahedra of the $I4/mmm$ structure about the *a*-axis of the *Bmab* structure such that the direction of rotation alternates between nearest neighbors in the basal planes. Neighboring octahedra in (100) planes are contrarotated, whereas those in (010) planes are corotated in the *Bmab* structure. The $P4_2/ncm$ structure is given from the parent structure by rotating the NiO_6 octahedra about $\langle 110 \rangle$ direction of the $P4_2/ncm$ structure in the basal plane such that nearest neighbors are contrarotated and the rotation axis alternates between [110] and [110] along the *c*-axis direction. The orthorhombic *Pccn* structure is visualized as a vector sum of the above two structures. Sullivan et al. [14] have prepared ten samples of $Pr_2NiO_{4+\delta}$, i.e., three $Pr_2NiO_{4.000}$ samples and seven samples of $Pr_2NiO_{4.020}$, $Pr_2NiO_{4.052}$, $Pr_2NiO_{4.064}$, $Pr_2NiO_{4.162}$, $Pr_2NiO_{4.17}$, $Pr_2NiO_{4.195}$, $Pr_2NiO_{4.215}$, and examined the phases of the respective samples up to 300 K with a conventional and high resolution synchrotron X-ray diffraction technique. They reported that, at room temperature, $Pr_2NiO_{4.000}$ is in orthorhombic *Pccn* symmetry, $Pr_2NiO_{4.020}$ and $Pr_2NiO_{4.052}$ are two-phase mixtures of the orthorhombic *Pccn* phase and the tetragonal $P4_2/ncm$ phase, $Pr_2NiO_{4.064}$ is in tetragonal $P4_2/ncm$ symmetry, $Pr_2NiO_{4.162}$ is a two-phase mixture of the tetragonal $P4_2/ncm$ phase and the orthorhombic $Fmmm(1)$ phase, $Pr_2NiO_{4.17}$ is in orthorhombic $Fmmm(1)$ symmetry, $Pr_2NiO_{4.195}$ is a two-phase mixture of the orthorhombic $Fmmm(1)$ phase and the orthorhombic $Fmmm(2)$ phase, and that $Pr_2NiO_{4.215}$ is in orthorhombic $Fmmm(2)$ symmetry. They presented a room temperature phase diagram of $Pr_2NiO_{4+\delta}$ prepared using above data. They also showed that $Pr_2NiO_{4+\delta}$ decomposes to $PrO_{1.83}$ and $Pr_4Ni_3O_7$, when $Pr_2NiO_{4+\delta}$ is annealed in pure oxygen below 1303 K.

In this paper, variation of the lattice constants at room temperature of $Nd_2NiO_{4+\delta}$ is reported as function of the excess oxygen concentration. Present crystal data of this study had shown that the room temperature phases of $Nd_2NiO_{4+\delta}$ are remarkably similar to the room temperature phases of $Pr_2NiO_{4+\delta}$ reported by Sullivan et al. [14] except that $Nd_2NiO_{4+\delta}$ is not decomposed to Nd_2O_3 and $Nd_4Ni_3O_7$ in pure oxygen. The similarities and the differences between the $Nd_2NiO_{4+\delta}$ phases, found in this work, and the $Pr_2NiO_{4+\delta}$ phases, reported by Sullivan et al. are reported in the paper.

2. Experimental

2.1. Preparative

The sample was prepared by a conventional solid state reaction. Reactants of Nd_2O_3 (Wako Pure Chemical Industries, 99.9%), which was heated in air at 1073 K for overnight to remove volatile impurities, and NiO (Kojundo Chemical Laboratory Co., 99.97%) were weighed to get the composition corresponding to $Nd_2NiO_{4+\delta}$. The weighed reactants were ground in an agate mortar, and the homogenized mixture was pelletized into pellets of 13 mm in diameter and 2 mm thick. These pellets were placed in an Al_2O_3 crucible and were heated in air at 1173–1473 K for 24–48 h. After the heating, the pellets were again ground, pelletized, and heated in the same condition. The grinding pelletizing heating cycle was repeated more than 6 times to get the sample.

The excess oxygen concentration of the as prepared sample was adjusted to predetermined value for successive measurements by either of the following procedures:

(A) An as prepared sample was heated in a flow of oxygen (0.1 MPa, 20 mL/min) at 1073 K for 2 h, and subsequently cooled in a flow of oxygen to 773 K at a cooling rate 3 K/min, to 373 K at 0.15 K/min, and to room temperature by radiation cooling. By this heat treatment, a sample in the range $0.22 \le \delta \le 0.224$ was obtained.

(B) An as prepared sample was heated in a flow of air (0.1 MPa, 20 mL/min) at 1073 K for 2 h, and subsequently cooled in the flow of air to room temperature with the same temperature program used in the method (A). By this heat treatment, a sample in the range $0.215 \le \delta \le 0.22$ was obtained.

(C) A powder of the as prepared sample was placed in a porcelain crucible and heated in a box furnace at 1073 K for more than 2 h. The crucible with the powder was then pull out from the internal of the furnace to the external, and the powder was rapidly cooled to room temperature in a breeze of air. By this heat treatment, a sample in the range $0.19 \le \delta \le 0.205$ was obtained.

(D) A sample given by the method (A) or (C) was heated in a circulatory flow of helium in a closed system equipped with an oxygen getter (Cu wires heated at 973 K) and moisture getters (liquid nitrogen traps) at a predetermined degassing temperature in the range $643\,K \le T \le 1213\,K$. By this heat treatment, a sample in the range $0.067 \le \delta \le 0.18$ was obtained. The excess oxygen concentration of each sample obtained by the method is shown in Fig. 1 as a function of the degassing temperature.

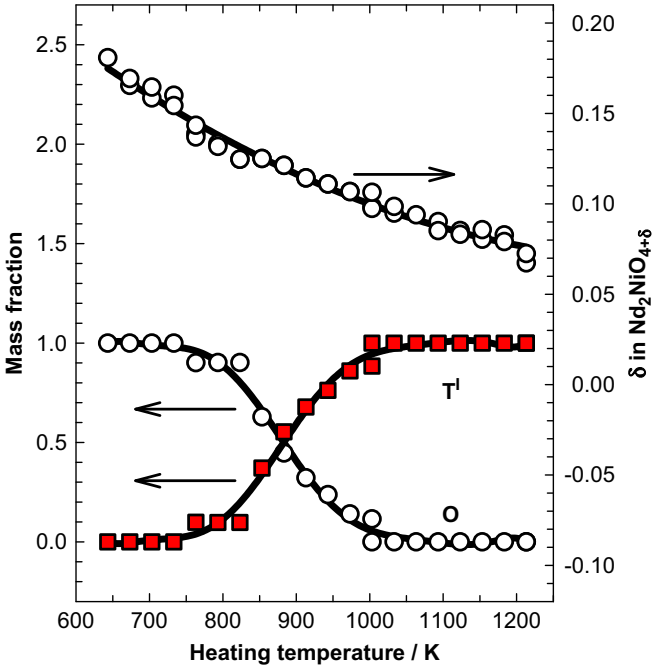

Fig. 1. Variations of the mass fractions of the orthorhombic and the quasi-tetragonal phases and the room temperature excess oxygen concentration of $Nd_2NiO_{4+\delta}$ with the degassing temperature in the range $643\,K \le T \le 1213\,K$. O: orthorhombic phase; T^I: quasi-tetragonal-I.

2.2. Chemical analyses

The excess oxygen concentration of each sample was determined by hydrogen reduction. A 5–9 g Pt-boat was repeatedly heated in air at 1073 K to constant weight. A 1–2 g sample was put on the Pt-boat and then repeatedly heated in air at 393 K to constant weight. The Pt-boat with the sample was again repeatedly heated in a circulatory flow of hydrogen at 973 K to constant weight with the same closed system used in the preparative section. The excess oxygen concentration of the sample was evaluated from the constant weights of the Pt-boat, the Pt-boat with the sample, and the Pt-boat with the reduced sample. On evaluating the concentration, the following reduction equation was assumed:

$$Nd_2NiO_{4+\delta} + (1+\delta)H_2 \rightarrow Nd_2O_3 + Ni + (1+\delta)H_2O.$$

All weighing was performed using Mettler–Toledo AG245 analytical balance with a readability of 0.01 mg. The analytical error occurring with the value of δ is 0.01, which is estimated from the dispersion of the concentration plots in Fig. 1.

2.3. X-ray powder diffraction measurements

X-ray powder diffraction data of each sample were collected in the range $10 \le 2\theta \le 104$ using a Rigaku RINT1200 X-ray diffractometer equipped with a Cu X-ray tube and a graphite monochromator. Just before or after the data collection of the sample, X-ray data of Si powder (Wako Pure Chemical Industries, 99.9%) were collected as an external standard in the range $22 \le 2\theta \le 100$. From the X-ray data, the phase purity and the lattice constants of the sample were confirmed and evaluated, respectively. A structure model for $La_2NiO_{4+\delta}$ proposed by Jorgensen et al. [33] was adopted for evaluating the lattice constants of $Nd_2NiO_{4+\delta}$: space group = *Fmmm*, $Z = 4$, Nd at 8*i* site (00*z*), Ni at 4*a* site (000), O1 at 8*e* site (1/41/40), O2 at 8*i* site (00*z*). A Rietveld software package of RIETAN-2000 [34] was used for the evaluations. It must be emphasized that this approach is used only to extract values of the lattice constants and does not imply that the respective phases are in the orthorhombic *Fmmm* symmetry. The true space group should be given only by accounting the tilts the NiO_6 octahedra and the distribution of the interstitial oxygen atoms in the crystal, which are not discussed in this paper.

When the X-ray diffraction data showed that a sample was a two-phase mixture of an orthorhombic phase and a quasi-tetragonal phase, the mass fractions of the respective phases were evaluated with the same program [34] using the method of Hill and Howard [35,36]. In this paper, the term of the quasi-tetragonal phase is used in the meaning that the phase is in orthorhombic symmetry, while the orthorhombic strain of the phase is very small. Since the two-phase mixture was found in the sample prepared by the method (D) of the preparative section, the mass fractions are shown in Fig. 1 as a function of the degassing temperature. Each sample is an orthorhombic phase in the ranges $643\,K < T \le 750\,K$ and $0.15 < \delta \le 0.181$, a quasi-tetragonal phase in the ranges $1020\,K < T \le 1213\,K$ and $0.067 \le \delta \le 0.10$, and a two-phase mixture in the ranges $750\,K < T \le 1020\,K$ and $0.10 < \delta \le 0.15$.

3. Results and discussion

Lattice constants and cell volume of each sample are shown in Fig. 2(a) and (b) as functions of the excess oxygen concentration, detailed crystal data are given in Table 1, and X-ray diffraction patterns of selected samples are shown in Fig. 3, respectively. In Fig. 2(a) and (b), both the lattice constants and the cell volume of each sample do not monotonously change with the value of δ. The spaces of Fig. 2(a) and (b) are, respectively, divided into five regions according to the variations with the excess oxygen concentration.

(A) In the range $0.21 < \delta \le 0.224$, an orthorhombic phase is existing. With increasing the value of δ, the lattice constant *a* decreases, the lattice constant *b* increases, and the lattice constant *c* increases. Mean value of the lattice constants *a* and *b*, i.e., (*a*+*b*)/2, slightly increases with increasing the value of δ. The cell volume

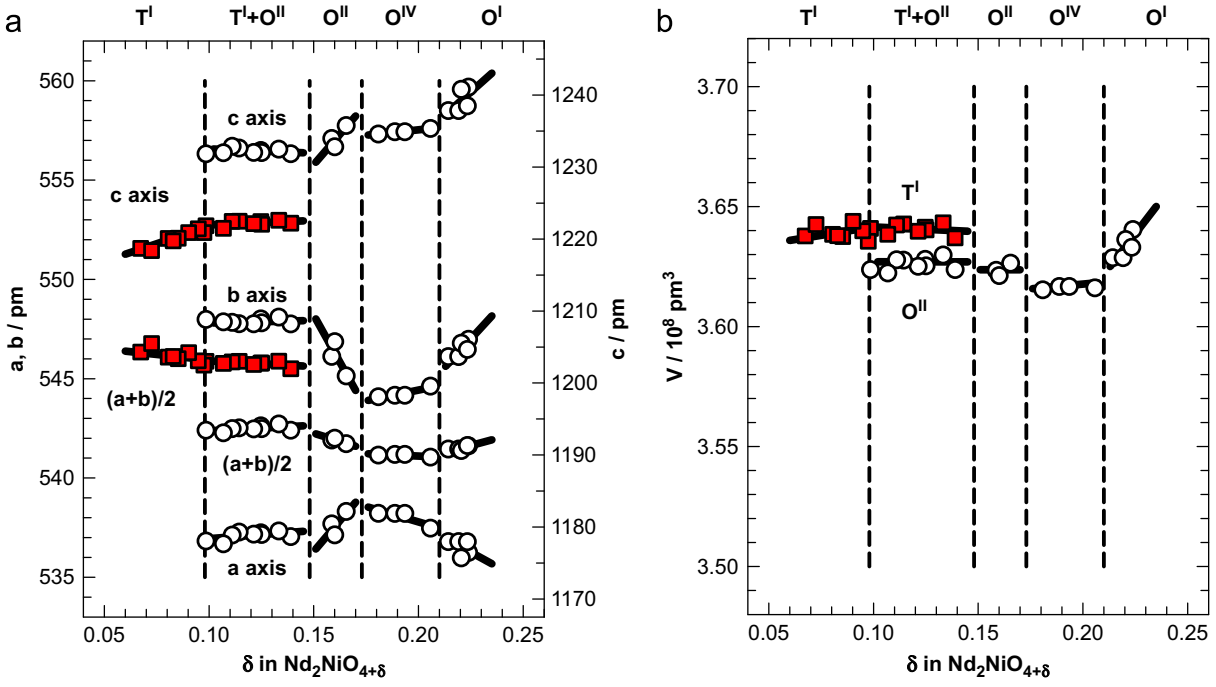

Fig. 2. Variation of (a) the lattice constants and (b) the cell volume at room temperature of $Nd_2NiO_{4+\delta}$ with the excess oxygen concentration. O^I: orthorhombic-I; O^{II}: orthorhombic-II; O^{IV}: orthorhombic-IV; T^I: quasi-tetragonal-I.

Table 1
Lattice constants in the condition of $a \le b \le c$ and cell volume of $Nd_2NiO_{4+\delta}$ at room temperature.

δ in $Nd_2NiO_{4+\delta}$	Phase	a (pm)	b (pm)	c (pm)	V (10^8 pm^3)
0.224	O^I	536.25(3)	546.98(3)	1241.10(7)	3.6404
0.223	O^I	536.79(2)	546.47(2)	1238.50(4)	3.6330
0.220	O^I	535.97(3)	546.79(3)	1240.79(7)	3.6363
0.219	O^I	536.79(1)	546.11(1)	1237.83(3)	3.6287
0.214	O^I	536.79(1)	546.11(1)	1237.83(3)	3.6287
0.206	O^{IV}	537.47(5)	544.62(5)	1235.36(11)	3.6161
0.193	O^{IV}	538.21(1)	544.16(1)	1234.90(2)	3.6167
0.189	O^{IV}	538.21(1)	544.16(1)	1234.90(2)	3.6167
0.181	O^{IV}	538.22(1)	544.08(1)	1234.58(3)	3.6153
0.165	O^{II}	538.31(1)	545.14(1)	1235.76(3)	3.6264
0.160	O^{II}	537.13(2)	546.87(2)	1232.81(4)	3.6212
0.159	O^{II}	537.69(2)	546.12(2)	1233.96(5)	3.6234
0.139[a]	O^{II}	537.04(1)	547.76(1)	1231.85(3)	3.6237
	T^I	545.50(6)		1222.20(16)	3.6369
0.133[a]	O^{II}	537.33(1)	548.10(1)	1232.49(3)	3.6298
	T^I	545.88(6)		1222.61(14)	3.6432
0.125[a]	O^{II}	537.15(2)	547.81(2)	1232.01(4)	3.6253
	T^I	545.79(3)		1222.05(6)	3.6403
0.125[a]	O^{II}	537.24(1)	548.01(1)	1232.29(3)	3.6280
	T^I	545.79(6)		1222.43(14)	3.6414
0.121[a]	O^{II}	537.17(2)	547.76(2)	1232.02(5)	3.6251
	T^I	545.72(3)		1222.15(4)	3.6397
0.114[a]	O^{II}	537.27(3)	547.77(3)	1232.64(6)	3.6277
	T^I	545.88(3)		1222.47(4)	3.6428
0.111[a]	O^{II}	537.12(3)	547.83(4)	1232.88(8)	3.6278
	T^I	545.85(3)		1222.46(4)	3.6423
0.107[a]	O^{II}	536.68(5)	547.86(6)	1231.98(12)	3.6223
	T^I	545.77(3)		1221.50(5)	3.6385
0.098[a]	O^{II}	536.82(6)	547.98(7)	1231.84(15)	3.6237
	T^I	545.88(3)		1221.85(4)	3.6409
0.097	T^I	545.36(3)	546.01(3)	1220.91(5)	3.6355
0.095	T^I	545.71(4)	546.09(4)	1221.43(7)	3.6399
0.090	T^I	546.11(4)	546.52(4)	1220.90(7)	3.6439
0.085	T^I	545.61(4)	546.42(4)	1220.12(8)	3.6375
0.083	T^I	545.79(4)	546.46(4)	1219.75(8)	3.6379
0.080	T^I	545.68(4)	546.50(4)	1220.09(8)	3.6384
0.073	T^I	546.18(4)	547.36(4)	1218.40(9)	3.6425
0.067	T^I	545.92(4)	546.77(4)	1218.71(8)	3.6378

The numbers in parentheses are the estimated standard deviations.In the single region, the lattice constants of the phase are evaluated with an orthorhombic *Fmmm* model.

[a] In the two-phase region, the lattice constants of the T^I phase are evaluated with a tetragonal *I*4/*mmm* model, and those of the O^{II} phase are evaluated with the orthorhombic *Fmmm* mode. The values of $\sqrt{2}a$ and $2V$ of the tetragonal *I*4/*mmm* cell are, respectively, shown as the lattice constants and the cell volume of the T^I phase.

rapidly increases with increasing the value of δ. This orthorhombic phase is called orthorhombic-I (O^I) in this paper. The O^I phase of $Nd_2NiO_{4+\delta}$ is corresponding to the *Fmmm*(2) phase of $Pr_2NiO_{4.215}$ reported by Sullivan et al. [14].

An X-ray diffraction pattern of $Nd_2NiO_{4.224}$ as an example of the O^I phase is shown in Fig. 3(a). The $Nd_2NiO_{4.224}$ sample is a well-crystallized polycrystalline powder. Most peaks are peaks from the O^I phase, while small unindexed peaks, whose positions are shown in Fig. 3(a) by downward pointing triangles, are found at $2\theta = 16.4^\circ$, 23.2°, 41.35°, and 42.0°. The peak at $2\theta = 16.4^\circ$ will be a peak from an amorphous phase, since the peak appears in a wide range $2\theta = 15.4$–17.4°. An integrated intensity of the peak at $2\theta = 16.4^\circ$ is I(peak, $2\theta = 15.4$–17.4°) = 2500 count, while a relative integrated intensity to baseline of the peak, i.e., I(peak, $2\theta = 15.4$–17.4°)/I(baseline, $2\theta = 15.4$–17.4°), is only 0.58, where a mean intensity of baseline is 22 count. Other unindexed peaks will be peaks from unknown crystalline phases, since the respective peaks appear in narrow ranges. The integrated intensities of the peaks at $2\theta = 23.2^\circ$, 41.35°, and 42.0° are I(peak, $2\theta = 22.8$–23.6°) = 580 count, I(peak, $2\theta = 41.0$–41.6°) = 300 count, and I(peak, $2\theta = 41.6$–42.4°) = 630 count, and the relative integrated intensities to baseline of the peaks are only 0.33, 0.30, and 0.46, respectively, where mean intensities of baselines are 17–22 count. No Nd_2O_3 peak, which will appear if exist at $2\theta = 26.864^\circ$ ($I/I_0 = 26\%$), 29.756° ($I/I_0 = 37\%$), 30.774° ($I/I_0 = 100\%$), 40.509° ($I/I_0 = 25\%$), 47.436° ($I/I_0 = 24\%$), 53.458° ($I/I_0 = 23\%$), and 57.004° ($I/I_0 = 19\%$) [37], is found in the X-ray diffraction pattern. No NiO peak, which will appear if exist at $2\theta = 37.249^\circ$ ($I/I_0 = 60\%$), 43.287° ($I/I_0 = 100\%$), 62.854° ($I/I_0 = 30\%$), and 62.914° ($I/I_0 = 25\%$) [38], is also found in the X-ray diffraction pattern. Sullivan et al. [14] reported that $Pr_2NiO_{4+\delta}$ decomposes to $PrO_{1.83}$ and $Pr_4Ni_3O_{10+\delta}$, when $Pr_2NiO_{4+\delta}$ is annealed in pure oxygen below 1303 K. Although $Nd_2NiO_{4.224}$ was prepared by annealing $Nd_2NiO_{4+\delta}$ in pure oxygen from 1073 K to room temperature, no Nd_2O_3 peak and no $Nd_4Ni_3O_{10-\delta}$ peak, which will appear if exist at $2\theta = 32.76^\circ$ ($I/I_0 = 100\%$) [39], are found in Fig. 3(a). The compound of $Nd_2NiO_{4+\delta}$ is stable in oxygen below 1073 K.

(B) In the range $0.175 < \delta \le 0.21$, an orthorhombic phase is existing. The values of a, b, c, and $(a+b)/2$ do not very change with the value of δ. Naturally, the cell volume does not very change with the value of δ. This orthorhombic phase is called orthorhombic-IV (O^{IV}) in this paper. The O^{IV} phase of $Nd_2NiO_{4+\delta}$ is corresponding to the two-phase mixture of the *Fmmm*(1) and the *Fmmm*(2) phases of $Pr_2NiO_{4.195}$ [14].

An X-ray diffraction pattern of $Nd_2NiO_{4.181}$ as an example of the O^{IV} phase is shown in Fig. 3(b). The $Nd_2NiO_{4.181}$ sample is well-crystallized powder. The O^{IV} phase of $Nd_2NiO_{4+\delta}$ is possibly a two-phase mixture of the O^I phase and the O^{II} phase given in (C) of this section, i.e., the two-phase mixture of the O^I phase of $Nd_2NiO_{4.21}$ and the O^{II} phase of $Nd_2NiO_{4.175}$. However, as shown in Fig. 2(a), because the expected lattice constants of the O^I phase of $Nd_2NiO_{4.21}$ and those of the O^{II} phase of $Nd_2NiO_{4.175}$ are almost identical, evidence of the two-phase mixture is not detected in Fig. 3(b) and in other X-ray diffraction patterns of the O^{IV} phase samples. Whether the O^{IV} phase is a two-phase mixture or a single phase is not concluded from the present data.

In Fig. 3(b), most peaks are peaks from the O^{IV} phase, while small unindexed peaks are found at $2\theta = 16.4^\circ$, 30.8°, and 41.2°. The peak at $2\theta = 16.4^\circ$ will be a peak from an amorphous phase, and the peak at $2\theta = 41.2^\circ$ will be a peak from an unknown crystalline phase. Integrated intensities of the two peaks are I(peak, $2\theta = 15.4$–17.6°) = 2400 count and I(peak, $2\theta = 40.8$–41.4°) = 300 count, while relative integrated intensities to baseline of the peaks are only 0.67 and 0.39, respectively, where mean intensities of baselines are 13–16 count. The peak at $2\theta = 30.8^\circ$ will be a peak from an unreacted starting material of Nd_2O_3. An integrated intensity, a relative integrated intensity to baseline, and a maximum peak intensity of the peak and a mean intensity of baseline are I(peak, $2\theta = 30.4$–31.1°) = 250 count, 0.22, 10–20 count, and 16 count, respectively. To estimate the amount of Nd_2O_3 in the sample, X-ray powder diffraction data of the starting material of Nd_2O_3 powder were collected with the same experimental condition that employed for the sample measurements. The integrated intensity and the maximum peak intensity of the peak at $2\theta = 30.8^\circ$ of the Nd_2O_3 powder are I(peak, $2\theta = 30.2$–31.4°) = 69 000 count and 3800 count, respectively. The integrated intensity data show that the $Nd_2NiO_{4.181}$ sample contains 0.36% of Nd_2O_3, and the peak height data show that the sample contains 0.26–0.52% of Nd_2O_3. Although the sample contains a trace amount of Nd_2O_3, no NiO peak is found in Fig. 3(b).

(C) In the range $0.15 < \delta \le 0.175$, an orthorhombic phase is existing. With increasing the value of δ, the value of a increases, the value of b decreases, and the value of c increases. The mean value of $(a+b)/2$ slightly decreases with increasing the value of δ. The cell volume does not very change with the value of δ. This

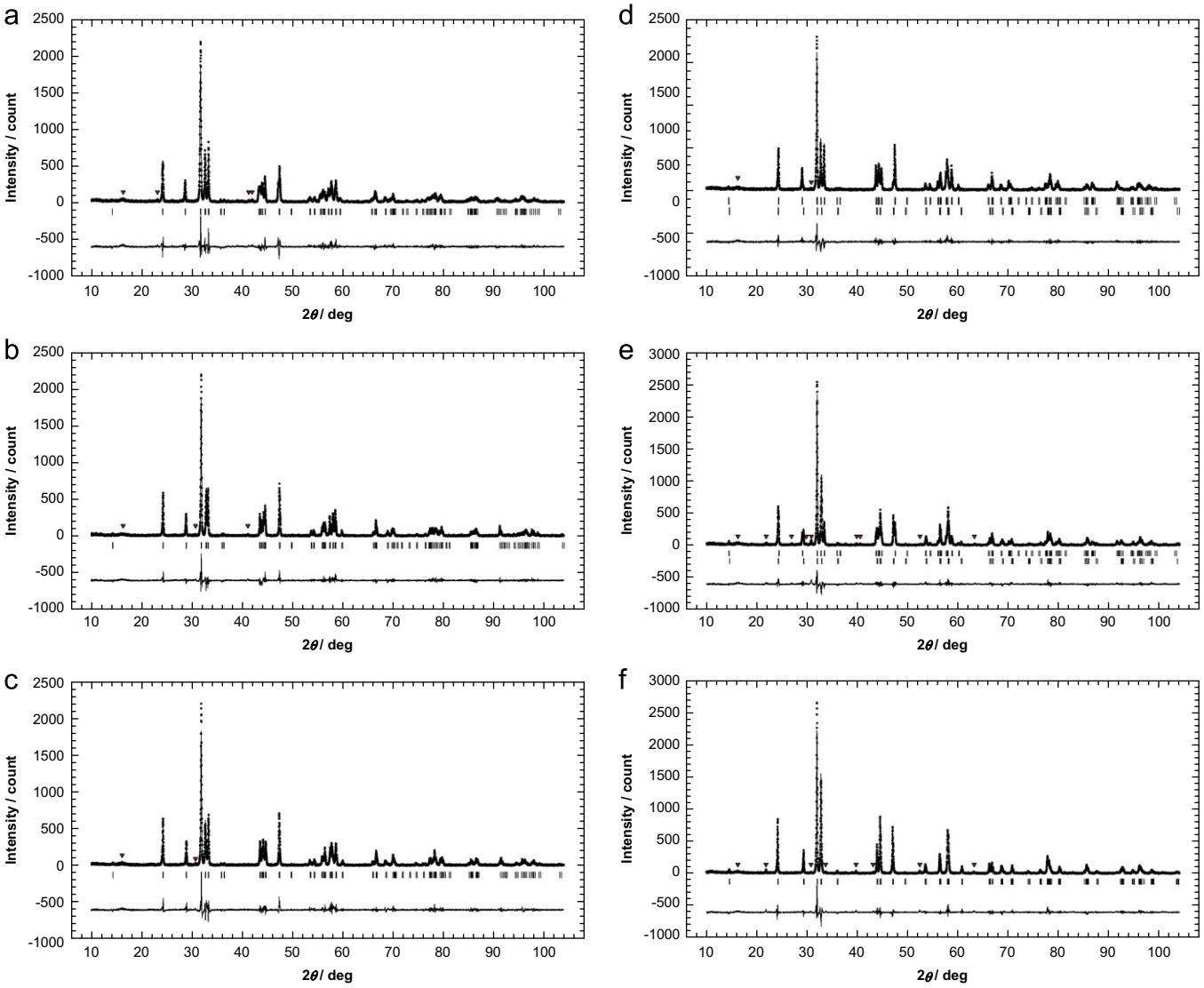

Fig. 3. X-ray powder diffraction patterns of (a) the O^{I} phase of $Nd_2NiO_{4.224}$, (b) the O^{IV} phase of $Nd_2NiO_{4.181}$, (c) the O^{II} phase of $Nd_2NiO_{4.160}$, (d) the two-phase mixture of the O^{II} phase (90.1%) and the T^{I} phase (9.9%) of $Nd_2NiO_{4.139}$, (e) the two-phase mixture of the O^{II} phase (44.7%) and the T^{I} phase (55.3%) of $Nd_2NiO_{4.121}$, and (f) the T^{I} phase of $Nd_2NiO_{4.067}$ at room temperature. Dots are the raw data. Solid lines are the calculated profiles. Thick marks below the profiles mark the positions of the allowed reflections. In (d) and (e), the upper and the lower thick marks mark the positions of the allowed reflections for the O^{II} and the T^{I} phases, respectively. Solid lines below the thick marks are the difference curves. The downward pointing triangles above the daw profiles correspond to impurity phases.

orthorhombic phase is called orthorhombic-II (O^{II}) in this paper. The O^{II} phase of $Nd_2NiO_{4+\delta}$ is corresponding to the *Fmmm*(1) phase of $Pr_2NiO_{4.17}$ [14].

An X-ray diffraction pattern of $Nd_2NiO_{4.160}$ as an example of the O^{II} phase is shown in Fig. 3(c). The $Nd_2NiO_{4.160}$ sample is well-crystallized powder. Most peaks are peaks from the O^{II} phase, while small unindexed peaks are found at $2\theta = 16.2^\circ$ and 30.8°. The peak at $2\theta = 16.2^\circ$ will be a peak from an amorphous phase. An integrated intensity of the peak is I(peak, $2\theta = 15.4$–17.6°) $= 2300$ count, while a relative integrated intensity to baseline of the peak is only 0.62, where a mean intensity of baseline is 17 count. The peak at $2\theta = 30.8^\circ$ will be a peak from the unreacted starting material of Nd_2O_3. An integrated intensity, a relative intensity to baseline, and a maximum peak intensity of the peak and a mean intensity of baseline are I(peak, $2\theta = 30.4$–31.1°) $= 320$ count, 0.62, 20 count, and 17 count, respectively. The integrated intensity data show that the sample contains 0.46% of Nd_2O_3, and the maximum peak intensity data show that the sample contains 0.52% of Nd_2O_3. Although the sample contains a trace amount of Nd_2O_3, no NiO peak is found in Fig. 3(c).

(D) In the range $0.10 < \delta \leq 0.15$, the O^{II} phase and the T^{I} phase given in (E) of this section are coexisting, i.e., the O^{II} phase of $Nd_2NiO_{4.15}$ and the T^{I} phase of $Nd_2NiO_{4.10}$ are coexisting. The two-phase mixture of the O^{II} phase and the T^{I} phase of $Nd_2NiO_{4+\delta}$ is corresponding to the two-phase mixture of the *Fmmm*(1) phase and the $P4_2/ncm$ phase of $Pr_2NiO_{4.162}$ [14], respectively. Although the $P4_2/ncm$ phase of $Pr_2NiO_{4+\delta}$ is in tetragonal symmetry, the T^{I} phase of $Nd_2NiO_{4+\delta}$ is, as discussed later in (E) of this section using the crystal data of the single phase region, not in tetragonal symmetry but in orthorhombic one. X-ray diffraction patterns of $Nd_2NiO_{4.139}$ and $Nd_2NiO_{4.121}$ as examples of the two-phase mixture are shown in Fig. 3(d) and (e), respectively. The $Nd_2NiO_{4.139}$ sample contains 90.1% of the O^{II} phase and 9.9% of the T^{I} phase, and $Nd_2NiO_{4.121}$ contains 44.7% of the O^{II} phase and 55.3% of the T^{I} phase. As shown in Fig. 3(d) and (e), the peaks from the T^{I} phase are almost completely superimposed on the peaks from the O^{II} phase. Initially, the lattice constants of the T^{I} phase and the O^{II} phase in this two-phase region had been tried to be determined simultaneously with an orthorhombic *Fmmm* model. However, the lattice constants of the T^{I} phase had incorrectly

converged to those of the O^{II} phase and had not been correctly obtained in this two-phase region, because the peaks from both phases are too completely superimposed. Thus, only in this two-phase region, the lattice constant c and the mean lattice constant $(a+b)/2$ of the T^{I} phase are evaluated with a tetragonal $I4/mmm$ model, and the lattice constants of the O^{II} phase are evaluated with the orthorhombic $Fmmm$ mode. In Fig. 2(a), the values of a, b, c, and $(a+b)/2$ of the O^{II} phase and the values of c and $(a+b)/2$ of the T^{I} phase are plotted. Naturally, in a two-phase region, the lattice constants and the cell volume of each phase do not change with the nominal composition of δ. The lattice constants of the T^{I} phase in this two-phase region should be truly equal to those of the T^{I} phase of $Nd_2NiO_{4.10}$ and be practically equal to those of $Nd_2NiO_{4.0975}$ given in Table 1, i.e., $a = 545.36$ pm, $b = 546.01$ pm, $c = 1220.91$ pm, and $(a+b)/2 = 545.685$ pm. Evaluated values of $(a+b)/2$ and c of the T^{I} phase in this two-phase region with the $I4/mmm$ model are in the range $545.50\,\text{pm} \le (a+b)/2 \le 545.88$ pm and $1221.50\,\text{pm} \le c \le 1222.61$ pm.

In Fig. 3(d), most peaks are peaks from the O^{II} and the T^{I} phases, while a few small unindexed peaks are found at $2\theta = 16.2^\circ$ and 30.8°. The peak at $2\theta = 16.2^\circ$ will be a peak from an amorphous phase. An integrated intensity of the peak is $I(\text{peak}, 2\theta = 15.2\text{–}17.2^\circ) = 2000$ count, while a relative intensity to baseline of the peak is only 0.57, where a mean intensity of baseline is 18 count. The peak at $2\theta = 30.8^\circ$ will be a peak from the unreacted starting material of Nd_2O_3. An integrated intensity, a relative integrated intensity to baseline, and a maximum peak intensity of the peak and a mean intensity of baseline are $I(\text{peak}, 2\theta = 30.6\text{–}31.1^\circ) = 200$ count, 0.26, 20 count, and 16 count, respectively. The integrated intensity data show that the $Nd_2NiO_{4.139}$ sample contains 0.29% of Nd_2O_3, and the maximum peak intensity data show that the sample contains 0.53% of Nd_2O_3. Although the sample contains a trace amount of Nd_2O_3, no NiO peak is found in Fig. 3(d).

In Fig. 3(e), most peaks are peaks from the O^{II} and the T^{I} phases, while many small unindexed peaks are found at $2\theta = 16.2^\circ$, 21.8°, 26.85°, 29.8°, 30.8°, 39.8°, 40.5°, 52.4°, and 63.2°. The peak at $2\theta = 16.2^\circ$ will be a peak from an amorphous phase. An integrated intensity of the peak is $I(\text{peak}, 2\theta = 15.2\text{–}17.4^\circ) = 2700$ count, while a relative integrated intensity to baseline of the peak is only 0.70, where a mean intensity of baseline is 17 count. The peaks at $2\theta = 21.8^\circ$, 39.8°, 52.4°, and 63.2° will be peaks from unknown crystalline phases. Integrated intensities of these unindexed peaks are $I(\text{peak}, 2\theta = 21.5\text{–}22.4^\circ) = 750$ count, $I(\text{peak}, 2\theta = 39.6\text{–}40.2^\circ) = 370$ count, $I(\text{peak}, 2\theta = 52.2\text{–}52.8^\circ) = 370$ count, and $I(\text{peak}, 2\theta = 63.0\text{–}63.6^\circ) = 310$ count, and relative integrated intensities to baseline of the peaks are 0.53, 0.47, 0.51, and 0.45, respectively, where mean intensities of baselines are 11–16 count. The peaks at $2\theta = 26.85^\circ$, 29.8°, 30.8°, and 40.5° will be peaks from Nd_2O_3. An integrated intensity, a relative intensity to baseline, and a maximum peak intensity of the peak at $2\theta = 30.8^\circ$ and a mean intensity of baseline are $I(\text{peak}, 2\theta = 30.2\text{–}31.0^\circ) = 1600$ count, 1.2, 70 count, and 17 count, respectively. The integrated intensity data show that the $Nd_2NiO_{4.121}$ sample contains 2.3% of Nd_2O_3, and the maximum peak intensity data show that the sample contains 1.8% of Nd_2O_3. In the midst of the two-phase region, the $Nd_2NiO_{4.121}$ sample contains an appreciable amount of Nd_2O_3, while no NiO peak is found in Fig. 3(e).

This amount of Nd_2O_3 in the $Nd_2NiO_{4.121}$ sample cannot be the unreacted starting material. Buttrey and Honig [40] reported that $Nd_2NiO_{4+\delta}$ decomposes to form Nd_2O_3 and NiO under sufficiently reducing conditions, while Saez-Puche et al. [21] had later denied this occurrence. The experimental data of this paper agree with the report of Buttrey and Honig [40], while no NiO peak is found in Fig. 3(e). The $Nd_2NiO_{4.139}$ sample in Fig. 3(d) prepared by heating $Nd_2NiO_{4+\delta}$ in a flow of helium at 763 K contains a trace amount of Nd_2O_3, and the $Nd_2NiO_{4.121}$ sample in Fig. 3(e) prepared by the same manner at 883 K contains an appreciable amount of Nd_2O_3. These experimental data suggest that $Nd_2NiO_{4+\delta}$ does not decompose to form Nd_2O_3 at 763 K but decomposes to form Nd_2O_3 at 883 K. However, as shown later in (E) of this section, $Nd_2NiO_{4+\delta}$ does not decompose to form Nd_2O_3 at 1213 K. The formation of Nd_2O_3 from $Nd_2NiO_{4+\delta}$ will occur in a limited temperature range. Although no NiO peak is found in Fig. 3(e), NiO may exist as an amorphous phase or microcrystals in this sample.

An equation for the decomposition reaction is as follows:

$$Nd_2NiO_{4+\delta} \rightarrow (1-x)Nd_2NiO_{4+\delta'} + xNd_2O_3 + xNiO,$$

$$\delta' = \delta/(1-x),$$

where δ is the nominal excess oxygen concentration of the $Nd_2NiO_{4+\delta}$ sample whose value is determined by hydrogen reduction, x is the Nd_2O_3 or NiO concentration in the sample, and δ' is the true excess oxygen concentration of $Nd_2NiO_{4+\delta'}$. The value of δ' is determined by the values of δ and x. In the case of the $Nd_2NiO_{4.121}$ sample in Fig. 3(e), the values of δ, x, and δ' are $\delta = 0.121$, $x = 0.018\text{–}0.023$, and $\delta' = 0.123\text{–}0.124$, respectively. Because the $Nd_2NiO_{4.121}$ sample is a mixture of 44.7% of the O^{II} phase of $Nd_2NiO_{4.15}$ and 55.3% of the T^{I} phase of $Nd_2NiO_{4.10}$, the value of δ' expected from the concentrations of the O^{II} phase and the T^{I} phase is 0.122. The values of δ, δ' expected from the values of δ and x, and δ' expected from the concentrations of the O^{II} phase and the T^{I} phase are almost the same.

Another explanation for Nd_2O_3 peaks but no NiO peak is possible. Choisnet et al. [41] and Odier et al. [42] reported the presence of $La_{2-x}NiO_{4+\delta}$, e.g., $La_{1.9}NiO_{3.93}$. Although the existence $Nd_{2-x}NiO_{4+\delta'}$ is not reported, if $Nd_{2-x}NiO_{4+\delta'}$ exists, $Nd_2NiO_{4+\delta}$ can form Nd_2O_3 without forming NiO by the following disproportionation reaction:

$$Nd_2NiO_{4+\delta} \rightarrow Nd_{2-x}NiO_{4+\delta'} + 0.5xNd_2O_3,$$

$$\delta' = \delta - 1.5x,$$

where δ is the nominal excess oxygen concentration of the $Nd_2NiO_{4+\delta}$ sample, x is the concentration of the Nd^{3+} vacancies in $Nd_{2-x}NiO_{4+\delta'}$ or twice the Nd_2O_3 concentration, and δ' is the true excess oxygen concentration of $Nd_{2-x}NiO_{4+\delta'}$. The value of δ' is determined by the values of δ and x. In the case of the $Nd_2NiO_{4.121}$ sample, the values of δ, x, and δ' are $\delta = 0.121$, $x = 0.036\text{–}0.046$, and $\delta' = 0.052\text{–}0.067$, respectively. The value of δ' in $Nd_{2-x}NiO_{4+\delta'}$ is considerably smaller than the value of δ in $Nd_2NiO_{4+\delta}$ and is not in the two-phase region of $Nd_2NiO_{4+\delta}$ in the range $0.10 < \delta \le 0.15$. Such a large change in the excess oxygen concentration may cause a change in the value of the lattice constant c of the O^{II} phase or the T^{I} phase in the sample, because $Nd_2NiO_{4+\delta}$ or $Nd_{2-x}NiO_{4+\delta'}$ is a layered compounds. However, as shown in Fig. 2(a) and Table 1, the values of c of the O^{II} phase and the T^{I} phase are in the range $1231.84\,\text{pm} \le c \le 1232.88$ pm and $1221.50\,\text{pm} \le c \le 1222.61$ pm, respectively, and both values of c are kept constants in this two-phase region. The effect of the Nd_2O_3 concentration on the lattice constants is not found in Fig. 2(a) and Table 1. Further investigation is necessary for the existence of $Nd_{2-x}NiO_{4+\delta'}$.

(E) In the range $0.067 \le \delta \le 0.10$, an orthorhombic phase exists. This orthorhombic phase is called quasi-tetragonal-I (T^{I}) in this paper. The T^{I} phase of $Nd_2NiO_{4+\delta}$ corresponds to the $P4_2/ncm$ phase of $Pr_2NiO_{4.064}$ [14]. While the $P4_2/ncm$ phase of $Pr_2NiO_{4.064}$ is in tetragonal symmetry, the T^{I} phase of $Nd_2NiO_{4+\delta}$ is apparently in orthorhombic symmetry. The lattice constants of the T^{I} phase evaluated with the $Fmmm$ model are given in Table 1. Standard deviations of the lattice constants a and b of the T^{I} phase are respectively 0.04 pm, and the values of $(b-a)$ of the T^{I} phase are in

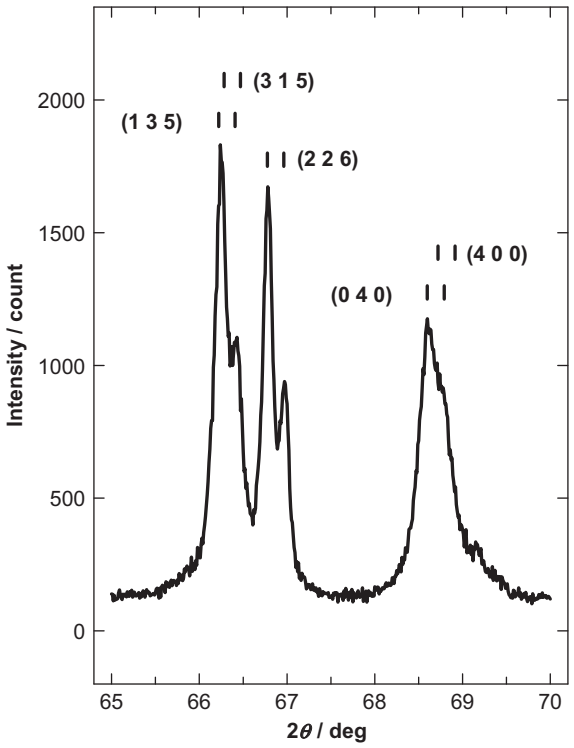

Fig. 4. X-ray powder diffraction patterns of the T^{I} phase of $Nd_2NiO_{4.073}$ at room temperature.

the range 0.38–0.85 pm. Above statistical data show that the T^{I} phase is in orthorhombic symmetry, as Takeda et al. have pointed out for the *Bmab* phase [30]. To confirm that the T^{I} phase is not in tetragonal symmetry, X-ray powder diffraction data of $Nd_2NiO_{4.073}$ were collected in the range $65 \leq 2\theta \leq 70$ with long counting time of 20 s. X-ray diffraction pattern of $Nd_2NiO_{4.073}$ are shown in Fig. 4. Although the (226) peaks are composed of two peaks, i.e., the peak from the Cu$K\alpha$1 radiation and the peak from the Cu$K\alpha$2 radiation, the (040) peak and the (400) peak superimpose to produce a single wider peak. Apparently, spacings of the (400) and the (040) planes are not the same, and thus the T^{I} phase is not in tetragonal symmetry. As noted in the introduction section, Buttrey et al. [13] have pointed out that space groups of *Bmab*, $P4_2/ncm$, and *Pccn* are given from the parent $I4/mmm$ structure by rotating the NiO_6 octahedra of the $I4/mmm$ structure. The small orthorhombic distortion of the T^{I} phase suggests that the T^{I} phase is in orthorhombic *Pccn* symmetry, when the parent structure is the undistorted $I4/mmm$ structure. The small orthorhombic distortion of the T^{I} phase can also be caused by the distortion of the parent $I4/mmm$ structure, i.e., the distortion of the NiO_6 octahedra. Puche et al. [21] reported the *Bmab* structure of Nd_2NiO_4. In this *Bmab* structure of Nd_2NiO_4, the NiO_6 octahedra are distorted in the *Bmab* structure, i.e., the oxygen–oxygen distances in the basal plane of a NiO_6 octahedron of the *Bmab* structure of Nd_2NiO_4 are 269.07 and 280.52 pm. The *Bmab* structure of Nd_2NiO_4 is not given from the $I4/mmm$ structure by rotating the NiO_6 octahedra of the $I4/mmm$ structure. The NiO_6 octahedra of $Nd_2NiO_{4+\delta}$ will be much easily distorted than that of $La_2NiO_{4+\delta}$ or $Pr_2NiO_{4+\delta}$, because the Goldshmidt tolerance factor of $Nd_2NiO_{4+\delta}$ is smaller than that of $La_2NiO_{4+\delta}$ or $Pr_2NiO_{4+\delta}$. In Table 1, the lattice constants of the T^{I} phase is given, but the values of a and b but $(a+b)/2$ are not plotted in Fig. 2(a), because the orthorhombic strain of the T^{I} phase is very small, and plotting the values of a and b with $(a+b)/2$ complicate the figure. In Table 1 and Fig. 2(a), the values of a, b, and $(a+b)/2$ slightly decrease with increasing the value of δ, but the value of c slightly increases with increasing the value of δ. In Fig. 2(b), the cell volume does not very change with the value of δ.

An X-ray diffraction pattern of $Nd_2NiO_{4.067}$ as an example of the T^{I} phase is shown in Fig. 3(f). Most peaks in Fig. 3(f) are peaks from the T^{I} phases. However, small but many peaks are found in Fig. 3(f) at $2\theta = 16.2^\circ$, 21.8°, 30.75°, 33.65°, 39.7°, 43.1°, 52.4°, and 63.2°. The peak at $2\theta = 16.2^\circ$ will be a peak from an amorphous phase. An integrated intensity of the peak is I(peak, $2\theta = 15.2$–$17.6^\circ) = 2600$ count, while a relative intensity to baseline of the peak is only 0.61, where a mean intensity of baseline is 18 count. The peaks at $2\theta = 21.8^\circ$, 33.65°, 39.7°, 43.1°, 52.4°, and 63.2° will be peaks from unknown crystalline phases. Integrated intensities of the peaks are I(peak, $2\theta = 21.4$–$22.2^\circ) =$ 640 count, I(peak, $2\theta = 30.4$–$34.0^\circ) = 550$ count, I(peak, $2\theta =$ 39.4–$40.1^\circ) = 620$ count, I(peak, $2\theta = 42.8$–$43.4^\circ) = 370$ count, I(peak, $2\theta = 52.0$–$52.8^\circ) = 908$ count, and I(peak, $2\theta =$ 62.8–$63.6^\circ) = 600$ count, and relative integrated intensities to baseline of the peaks are 0.43, 0.77, 0.74, 0.50, 1.1, and 0.70, respectively, where mean intensities of baselines are 11–19 count. The peak at $2\theta = 30.75^\circ$ will be a peak from the unreacted starting material of Nd_2O_3. An integrated intensity, a relative integrated intensity to baseline, and a maximum peak intensity of the peak and a mean intensity of baseline are I(peak, $2\theta = 30.4$–$31.2^\circ) = 97$ count, 0.076, 10 count, and 16 count, respectively. The integrated intensity data show that the $Nd_2NiO_{4.139}$ sample contains 0.14% of Nd_2O_3, and the maximum peak intensity data show that the sample contains 0.26% of Nd_2O_3. Although the sample contains a trace amount of Nd_2O_3, no NiO peak is found in Fig. 3(f).

In the examined range $0.067 \leq \delta \leq 0.224$, the orthorhombic *Bmab* phase with a large orthorhombic strain, reported by Puche et al. [21] and Carvajal et al. [22], was not observed. This phase may exist in the range $\delta \leq 0.067$, and thus the name of orthorhombic-III (O^{III}) is reserved for this phase in this paper for the continuing study.

Crystal data of the phases found at room temperature are compared below. In the O^{I}, O^{II}, O^{IV}, and T^{I} phases, the T^{I} phase is distinguished from the other phases for three reasons: (i) The orthorhombic strain of the T^{I} phase is remarkably smaller than that of the other phases. (ii) The value of $(a+b)/2$ of the T^{I} phase is much larger than that of the other phases. (iii) The value of c of the T^{I} phase is much smaller than that of the other phases. The structure of the T^{I} phase, i.e., the structure of the excess oxygen in the T^{I} phase should be different from that of the other phases.

In the O^{I}, O^{II}, O^{IV}, and T^{I} phases, the O^{I} phase is also distinguished from the other phases for a reason. The cell volume of the O^{I} phase rapidly increases with increasing the value of δ, while the cell volumes of the other phases do not change with the value of δ. In the O^{I} phase, a correlation among the excess oxygen atoms should be very strong.

In the O^{II}, O^{IV}, and T^{I} phases, the order of the cell volumes is unusual. Although the formula weights (FW) of the phases are arranged in order of the value $FW(T^{I}) < FW(O^{II}) < FW(O^{IV})$, the cell volumes ($V$) of the phases are arranged in order of the value $V(T^{I}) > V(O^{II}) > V(O^{IV})$. Naturally, the densities (ρ) and the filling rates (FR) of the phases are arranged in order of the value $\rho(T^{I}) < \rho(O^{II}) < \rho(O^{IV})$ and $FR(T^{I}) < FR(O^{II}) < FR(O^{IV})$, respectively. The structure of the excess oxygen in each phase should determine these orders.

4. Conclusions

In this study, variation of the room temperature phases of $Nd_2NiO_{4+\delta}$ with the excess oxygen concentration is examined. The sample is the O^{I} phase, the O^{IV} phase, the O^{II} phase, a two-phase

mixture of the O^{II} phase and the T^{I} phase, and the T^{I} phase in the ranges $0.21<\delta\leq0.224$, $0.175<\delta\leq0.21$, $0.15<\delta\leq0.175$, $0.10<\delta\leq0.15$, and $0.067\leq\delta\leq0.10$, respectively.

References

[1] C.N.R. Rao, D.J. Buttrey, N. Otsuka, P. Ganguly, H.R. Harrison, C.J. Sandberg, J.M. Honig, J. Solid State Chem. 51 (1984) 266–269.
[2] K. Ishikawa, W. Shibata, K. Watanabe, T. Isonaga, M. Hashimoto, Y. Suzuk, J. Solid State Chem. 131 (1997) 275–281.
[3] J.M. Bassat, P. Odier, A. Villesuzanne, C. Marin, M. Pouchard, Solid State Ionics 167 (2004) 341–347.
[4] H. Tamura, A. Hayashi, Y. Ueda, Physica C 216 (1993) 83–88.
[5] D.E. Rice, D.J. Buttrey, J. Solid State Chem. 105 (1993) 197–210.
[6] A. Hayashi, H. Tamura, Y. Ueda, Y. Takeda, J. Supercond. 7 (1994) 59–61.
[7] K. Yamada, T. Omata, K. Nakajima, Y. Endoh, S. Hosoya, Physica C 221 (1994) 355–362.
[8] H. Tamura, A. Hayashi, Y. Ueda, Physica C 258 (1996) 61–71.
[9] T. Kyomen, M. Oguni, M. Itoh, K. Kitayama, Phys. Rev. B 60 (1999) 815–821.
[10] T. Kyomen, M. Oguni, M. Itoh, K. Kitayama, Phys. Rev. B 60 (1999) 14841–14846.
[11] M. Hucker, K. Chung, M. Chand, T. Vogt, J.M. Tranquada, D.J. Buttrey, Phys. Rev. B 70 (2004) 064105.
[12] N. Poirot, P. Simon, P. Odier, Solid State Sci. 10 (2008) 186–192.
[13] D.J. Buttrey, J.D. Sullivan, G. Shirane, K. Yamada, Phys. Rev. B 42 (1990) 3944–3951.
[14] J.D. Sullivan, D.J. Buttrey, D.E. Cox, J. Hriljac, J. Solid State Chem. 94 (1991) 337–351.
[15] J.L. Martinez, M.T. Fernandez-Diaz, J. Rodriguez-Carvajal, P. Odier, Phys. Rev. B 43 (1991) 13766–13769.
[16] M.T. Fernandez-Diaz, J. Rodriguez-Carvajal, J.L. Martinez, G. Fillion, F. Fernandez, R. Saez-Puche, Z. Phys. B 82 (1991) 275–282.
[17] M.T. Fernandez-Diaz, J. Rodriguez-Carvajal, J.L. Martinez, P. Odier, Physica B 180–181 (1992) 122–124.
[18] M.T. Fernandez-Diaz, J.L. Martinez, J. Rodriguez-Carvajal, J. Beille, P. Odier, Phys. Rev. B 47 (1993) 5834–5840.
[19] C. Allancon, J. Rodriguez-Carvajal, M.T. Fernandez-Diaz, P. Odier, J.M. Bassat, J.P. Loup, J.L. Martinez, Z. Phys. B 100 (1996) 85–90.
[20] P. Odier, Ch. Allancon, J.M. Bassat, J. Solid State Chem. 153 (2000) 381–385.
[21] R. Saez-Puche, F. Fernandez, J.R. Carvajal, J.L. Martinez, Solid State Commun. 72 (1989) 273–277.
[22] J. Rodriguez-Carvajal, M.T. Fernandez-Diaz, J.L. Martinez, F. Fernandez, R. Saez-Puche, Europhys. Lett. 11 (1990) 261–268.
[23] F. Fernandez, R. Saez-Puche, M.T. Fernandez-Diaz, J. Rodriguez-Carvajal, J.L. Martinez, I.L. Botto, E.J. Baran, Euro. J. Solid State Inorg. Chem. 28 (1991) 507–5010.
[24] X. Batlle, B. Martinez, X. Obradors, M. Pernet, M. Vallet, J. Gonzalez-Calvet, J. Alonso, J. Mag. Mag. Mater. 104–107 (1992) 918–920.
[25] X. Batlle, X. Obradors, B. Martinez, Phys. Rev. B 45 (1992) 2830–2843.
[26] C.H. Chen, S.W. Cheong, D.J. Werder, H. Takagi, Physica C 206 (1993) 183–194.
[27] R. Burriel, M. Castro, R. Saez-Puche, Pure Appl. Chem. 67 (1995) 1825–1830.
[28] M. Castro, R. Burriel, Thermochim. Acta 269–270 (1995) 523–535.
[29] M.T. Fernandez-Diaz, R. Saez-Puche, Physica B 241–243 (1998) 364–366.
[30] Y. Takeda, M. Nishijima, N. Imanishi, R. Kanno, O. Yamamoto, M. Takano, J. Solid State Chem. 96 (1992) 72–83.
[31] S. Bhavaraju, J.F. DiCarlo, D.P. Scarfe, I. Yazdi, A.J. Jacobson, Chem. Mater. 6 (1994) 2172–2176.
[32] M. Zaghrioui, F. Giovannelli, N.P.D. Brouri, I. Laffez, J. Solid State Chem. 177 (2004) 3351–3358.
[33] J.D. Jorgensen, B. Dabrowski, S. Pei, D.R. Richards, D.G. Hinks, Phys. Rev. B 40 (1989) 2187–2199.
[34] F. Izumi, T. Ikeda, Mater. Sci. Forum 321–324 (2000) 198–203.
[35] R.J. Hill, C.J. Howard, J. Appl. Crystallogr. 20 (1987) 467–474.
[36] R.J. Hill, in: R.A. Young (Ed.), The Rietveld Method (International Union of Crystallography Monographs on Crystallography 5), Oxford University Press, Oxford, 1995, pp. 61–101.
[37] International Centre for Diffraction Data (ICDD), 41–1089.
[38] International Centre for Diffraction Data (ICDD), 44–1159.
[39] A. Olafsen, H. Fjellvasg, B.C. Hauback, J. Solid State Chem. 151 (2000) 46–55.
[40] D.J. Buttrey, J.M. Honig, J. Solid State Chem. 72 (1988) 38–41.
[41] J. Choisnet, J.M. Bassat, H. Pilliere, P. Odier, M. Leblanc, Solid State Commun. 66 (1988) 1245–1249.
[42] P. Odier, J.M. Bassat, J.C. Rifflet, J.P. Loup, Solid State Commun. 85 (1993) 561–564.